Trends in Global and Basin-Scale Runoff over the Late Twentieth Century: Methodological Issues and Sources of Uncertainty

R. ALKAMA, B. DECHARME, H. DOUVILLE, AND A. RIBES

CNRM-GAME, Météo-France, and CNRS, Toulouse, France

(Manuscript received 30 June 2010, in final form 27 December 2010)

ABSTRACT

While human influence has been detected in global and regional surface air temperature, detection–attribution studies of direct (i.e., land use and water management) and indirect (i.e., climate related) effects of human activities on land surface hydrology remain a crucial and controversial issue. In the present study, a set of global offline hydrological simulations is performed during the 1960–94 period using the Interactions between Soil, Biosphere, and Atmosphere–Total Runoff Integrating Pathways (ISBA-TRIP) modeling system. In contrast to previous numerical sensitivity studies, the model captures the observed trend in river runoff over most continents without including land use changes and/or biophysical CO_2 effects, at least when the comparison is made over 154 large rivers with a minimum amount of missing data. The main exception is northern Asia, where the simulated runoff trend is negative, in line with the prescribed precipitation forcing but in contrast with the observed runoff trend. The authors hypothesize that the observed surface warming and the associated decline of permafrost and glaciers, not yet included in most land surface models, could have contributed to the increased runoff at high latitudes. They also emphasize that the runoff trend is a regional-scale issue, if not basin dependent. In line with recent observational studies, their results suggest that CO_2 stomatal conductance effects and land use changes are not the primary drivers of the multidecadal runoff variability at continental scales. However, the authors do not rule out a human influence on land runoff, at least through the high-latitude surface warming observed over recent decades.

1. Introduction

While it is now very likely that the anthropogenic emissions of greenhouse gases have contributed to the observed twentieth-century global warming, and that this warming will amplify over the twenty-first century, the detection and attribution of the recent evolution of continental runoff is still an open question (Labat et al. 2004; Gedney et al. 2006, hereafter G06; Piao et al. 2007; Milliman et al. 2008; Gerten et al. 2008; Dai et al. 2009; Alkama et al. 2010b), and the twenty-first-century hydrological projections remain highly uncertain even at the global scale (e.g., Douville et al. 2006). Understanding the natural and anthropogenic contributions to the twentieth-century evolution of land runoff is a key issue for constraining the response of the land surface hydrology in twenty-first-century climate projections. Unfortunately, even the observed global trend remains unclear, given the scarcity and heterogeneity of river discharge measurements.

On the observational side, the direct measurement of streamflow discharge is difficult and water-surface elevation (stage) is generally used as a surrogate, using an empirical fit between stage measurements and concurrent river discharge. Such estimations can be in error, especially in the case of variable downstream channel conditions. Moreover, the length and reliability of the available time series vary greatly from one river basin to another, and gaps are usually found. To fill these gaps, either statistical or numerical simulations using land surface models (LSMs) are generally used. In any case, the more gaps there are to fill, the more uncertain the reconstructed runoff trends are.

Using data based on 221 rivers (corresponding to roughly 50% of the global land drainage area) and a statistical wavelet method to estimate missing runoff observations (RoL), Labat et al. (2004) documented a significant increase in global runoff over the twentieth century. Wavelets, like other time series methods, can be useful in data smoothing applications and for unbiased estimations of

Corresponding author address: Ramdane Alkama, CNRM-GAME, Météo-France, 42 ave. G. Coriolis, 31057 Toulouse, France.
E-mail: ramdane.alkama@cnrm.meteo.fr

DOI: 10.1175/2010JCLI3921.1

short runs of missing data when a significant trend is present (Soon et al. 2004); however, this method is probably less appropriate when data are missing for long periods. For most gauging stations, only a few decades of data exist and, in some cases, less than 10 yr are available. In consequence, considerable uncertainty is introduced in the reconstructed time series when a large fraction of the data is statistically derived. For all these reasons, Legates et al. (2005) argue that the estimation errors introduced by the wavelet transform method are large enough to call the results of Labat et al. (2004) into question. In a recent study, Milliman et al. (2008) analyzed cumulative annual discharge from 137 representative rivers to the global ocean and did not find any global trend. A number of high-latitude rivers were, however, shown to experience increased discharge despite declining precipitation. The study suggested that this paradox could not be fully explained by poorly constrained meteorological and hydrological data, and that changes in discharge seasonality and decreased storage may also play important roles. More recently, Dai et al. (2009) used a LSM in offline mode to fill the gaps in the observed discharge time series over 925 rivers and found no significant trend during the 1948–2004 period. They also pointed out a large upward trend in the yearly discharge into the Arctic Ocean.

Besides these observational studies, there have been several numerical studies aimed at explaining the twentieth-century global runoff increase reported by Labat et al. (2004). Using the Met Office Surface Exchange Scheme (MOSES) LSM in offline mode, G06 suggested that the stomatal closure effect associated with increasing atmospheric CO_2 was mainly responsible for the positive trend during the 1960–94 period. Using the same hydrology coupled to an atmospheric general circulation model, Betts et al. (2007) confirmed the relevance of this stomatal closure effect in doubled CO_2 experiments and further showed that it could not be offset by the CO_2 fertilization effect in this model. In contrast, Huntington (2008) provided evidence from independent observations that transpiration has not decreased, thereby refuting the G06 suggestion. Moreover, using an experiment design similar to that of G06 but with the Organizing Carbon and Hydrology in Dynamic Ecosystems (ORCHIDEE) LSM, Piao et al. (2007) found compensation between the stomatal closure and fertilization effects. They attributed half of the twentieth-century global positive runoff trend to a land use effect and the other half to the prescribed atmospheric forcings. They nevertheless compared their global simulations (100% of land area) with the runoff reconstruction of Labat et al. (2004) that encompasses only 50% of the total drainage area. More recently, using the Lund–Potsdam–Jena managed land (LPJmL) model, Gerten et al. (2008) attributed +70%, +19%, +14%, and −3% of the global positive trend to changes in climate (precipitation + temperature), land use, CO_2 (fertilization + stomatal conductance effect), and irrigation, respectively. The relative importance of the fertilization and stomatal closure effects and of changes in land use is still very model dependent (Alkama et al. 2010b).

Understanding the multidecadal variability of observed runoff is therefore of great importance to better constrain LSMs used in global and regional climate scenarios. Such models can indeed be driven by reconstructed atmospheric forcings to try to replicate the observed runoff trends. This approach, however, raises a number of methodological issues: atmospheric forcings must be as homogeneous as possible and the comparison with observed runoff must be limited to the river basins where long and reliable time series of discharge observations are available and are not much directly influenced by human activities (i.e., damming and irrigation). The main goal of the present study is to assess the ability of a ''state of the art'' LSM to capture the observed runoff trends over the second half of the twentieth century. Another objective is to discuss the possible limitations of former similar studies (e.g., G06; Piao et al. 2007; Dai et al. 2009) and to suggest an alternative explanation for the apparent contradiction between observed precipitation and runoff trends at the continental scale. Indeed, in some previous studies (i.e., G06; Piao et al. 2007; Gerten et al. 2008), only the global averaged—or at least continent by continent—simulated runoff trends have been evaluated. Thus, it has not been possible to identify the basins with a significant mismatch between simulated and observed runoff trends. In the present study, we perform a basin-by-basin comparison of 154 river basins without gaps in the monthly discharge time series during the entire 1960–94 period.

To reach these objectives, the Interactions between Soil, Biosphere, and Atmosphere–Total Runoff Integrating Pathways (ISBA-TRIP) Continental Hydrological System (CHS) is driven using a hybrid global atmospheric forcing combining 3-hourly meteorological analyses and monthly observations over the second half of the twentieth century (Sheffield et al. 2006). Besides the default full Global Precipitation Climatology Centre (GPCC) data product, the Variability Analysis of Surface Climate Observations (VASClimO) dataset from the Global Precipitation Climatology Center (GPCC) is used as an alternative precipitation forcing to evaluate the relevance of data homogeneity for continental-scale runoff simulations. This product uses only the station time series with a minimum of 90% data availability during the 1948–2000 periods to minimize the risk of temporal inhomogeneities due to varying station density. This precipitation dataset is therefore more reliable for land precipitation–runoff

trend analyses. The ISBA-TRIP CHS, the global atmospheric forcing, the land surface parameters, and the experiment design are described in section 2. The main results are presented in section 3. A sensitivity study to input precipitation forcing is given in section 4. Finally, a discussion and the main conclusions are provided in sections 5 and 6, respectively.

2. Model and experiment design

a. ISBA-TRIP model

The model used for this study uses the ISBA-TRIP CHS (Alkama et al. 2010a). ISBA is the land surface model of Météo-France. It is a process-based force–restore method (Noilhan and Planton 1989) to calculate the time evolution of the surface energy and water budgets, including snowpack evolution based on a one-layer scheme (Douville et al. 1995). The soil hydrology is represented by three layers (a thin surface layer included in the rooting layer and a third layer to distinguish between the rooting depth and the total soil depth), which ensure the vertical water exchange between the land surface and the atmosphere (Boone et al. 1999). The soil water content varies with surface infiltration, soil evaporation, plant transpiration, and deep drainage. The infiltration rate is computed as the difference between the throughfall rate and the surface runoff. The throughfall rate is the sum of rainfall not intercepted by the canopy, dripping from the interception reservoir and snowmelt from the snowpack. A comprehensive parameterization of subgrid hydrology to account for the heterogeneity of precipitation, topography, soil depth, and vegetation within each grid cell is used to improve the ISBA's runoff simulation (Decharme and Douville 2006, 2007). Every day of the simulation, this total runoff (surface runoff + deep drainage) simulated by ISBA is fed into TRIP (Oki and Sud 1998), which is integrated with a 1-h time step at 0.5° resolution. TRIP is a river routing model used to convert the daily runoff simulated by ISBA into river discharge on the global river channel network. It is a simple linear model based on a single prognostic equation for the water mass within each grid cell of the hydrologic network.

It is important to note that the ISBA-TRIP CHS has been intensively validated at global scale during the recent period (1986–2006) by comparing simulations to in situ river discharges and terrestrial water storage (TWS) from three Gravity Recovery and Climate Experiment (GRACE) products (Decharme and Douville 2007; Decharme 2007; Alkama et al. 2010a). Indeed, the results of these studies have shown that, in general, ISBA-TRIP successfully captures the seasonal and the interannual variability in both TWS and discharges.

b. Forcing data and land surface parameters

Note first that we only focus on the climate forcing of the land surface hydrology, so that other anthropogenic effects than climate change (direct CO_2 impacts on evapotranspiration, land use, groundwater, dams, and irrigation) are not considered. The 1° resolution global meteorological forcing dataset from Princeton University (Sheffield et al. 2006) contains 3-hourly time step precipitation, temperature, humidity, surface downward shortwave and longwave radiation, wind speed, and surface pressure (http://hydrology.princeton.edu). This dataset is based on the National Centers for Environmental Prediction–National Center for Atmospheric Research (NCEP–NCAR) reanalyses. Sheffield et al. (2006) have corrected the systematic biases in the 6-hourly NCEP–NCAR reanalyses via hybridization with global monthly gridded observations. In addition, the precipitation is disaggregated in both space and time at 1° resolution via statistical downscaling and at a 3-hourly time step using information from the 3-hourly Tropical Rainfall Measuring Mission (TRMM) dataset. More detail on this forcing product can be found in Sheffield et al. (2006). In this study, the 3-hourly precipitation from Sheffield et al. (2006) was hybridized to match the monthly values from the VASClimO GPCC precipitation dataset. This dataset supplied gridded time series for studies on climate variability, for example, an analysis of long-term trends. For this gridded data, only (mostly) complete data time series were used after quality control and homogeneity tests (Beck et al. 2005). As already stated, this precipitation dataset is particularly reliable for land precipitation–runoff long-term trend studies.

The land surface parameters were specified according to the 1-km-resolution ECOCLIMAP database developed at Météo-France (Masson et al. 2003). The soil textural properties were given by the Food and Agriculture Organization (FAO) map at 10-km resolution. Vegetation parameters were defined using two vegetation datasets: the Coordination of Information on the Environment (CORINE) land cover archive at 250-m resolution over Europe and the University of Maryland (Hansen et al. 2000) dataset at 1 km elsewhere. The mean grid cell elevation was specified according to the 30 arc-second-resolution (GTOPO30) dataset (http://eros.usgs.gov/products/elevation/gtopo30/gtopo30.html).

c. Model setup and experiments

ISBA was integrated at 1° resolution with a 20-min time step for 1948–2000, where the first 2 yr were considered as spinup. Therefore, only 1960–94 was used in the runoff trend analysis. The ISBA total runoff is interpolated from 1° to 0.5° before being fed into TRIP. On the one hand, we

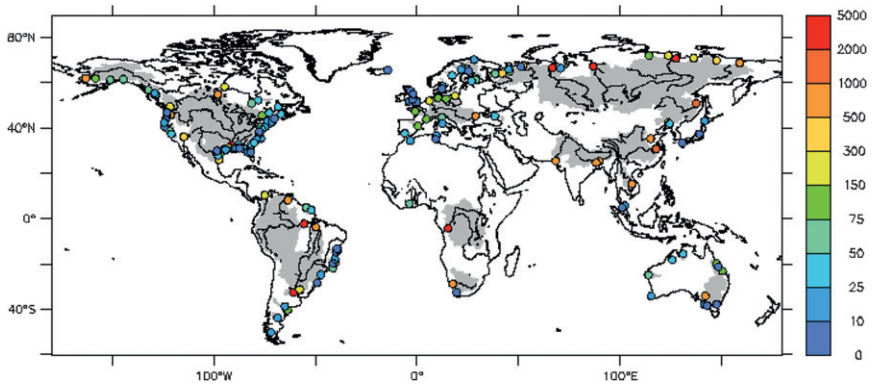

FIG. 1. Distribution of the farthest downstream gauge stations for the 154 representative rivers included in this study from Dai et al. (2009) during the 1960–94 period. The color of the dots indicates the observed values of the drainage area (10^3 km^2) at each gauge stations, while the gray color gives an idea of the total drainage area represented in this study (about 33% of the global land surface).

analyzed the simulated runoff (RsG) trends averaged over the total land area over the globe and/or each continent. On the other hand, we compared the simulated runoff trends to the observationally based dataset from Dai et al. (2009) over the same drainage area that was delimited by the in situ gauge station (gray patterns in Fig. 1).

In any case, the more gaps to be filled, the more uncertain the reconstructed runoff trends are. This is why in the present study we chose to focus only on the rivers without gaps during the entire 1960–94 period, that is, a total of 154 rivers that represent 41% of the global land runoff and at least 33% of the total river basin area. This fraction differs from one continent to another: it is only about 20% over Africa, whereas it represents about 70% of the total area over North America. Our catchment area estimates were derived from the 0.5° × 0.5° TRIP river channel network (corresponding to a 3% change globally between the simulated and observed global river basins area). The global mean TRIP drainage area for the entire 1960–94 study period was 44 compared to 43 10^6 km^2 in observations. Figure 1 shows the observed drainage area at the 154 in situ gauging stations selected in this study. The spatial density of the gauging stations is contrasted over the different continents, with only 7 stations over Africa and a maximum number of 50 and 32 stations over North America and Europe, respectively.

d. Statistical method used in this study

This study is widely based on trend analysis. Throughout the paper, trends are calculated with respect to the linear Gaussian model. In particular, this model assumes that the observation y_j performed at time t_i satisfies

$$y_i = at_i + b + \varepsilon_i, \tag{1}$$

where ε_i are independent, identically distributed Gaussian random variables.

Within this statistical framework, the trend (i.e., the coefficient a) is estimated by $\hat{a}$, via the ordinary least squares method, and so is the variance of ε_i, called σ. Then, the linear model presented before allows for the calculation of confidence intervals and hypothesis testing about this trend, based on the Student's t distribution. Confidence intervals are used to illustrate the uncertainty on the estimated trend; this study illustrates that this uncertainty is often large when trends are computed during a relatively short period (35 yr).

Hypothesis testing procedures are implemented for testing the hypothesis H_0 ($a = 0$) versus H_1 ($a \neq 0$). Under this null hypothesis H_0, $\hat{a}/\hat{\sigma}$ follows a Student's distribution with $n - 2$ degrees of freedom up to a scalar factor. This result is used to compute the p value of the test. Note that in statistical hypothesis testing, the p value is the probability of obtaining a test statistic at least as extreme as the one actually observed, assuming that the null hypothesis is true. The lower the p value, the less likely the result is if the null hypothesis is true. The p value criterion will be widely used to demonstrate how much the estimated trends are different from 0. In the following, we chose the values 0.1, 0.05, and 0.01 as a threshold for representing the p values. One can note that a p value <0.05 indicates a trend that is significant at the 0.95 level. Thus, we chose to focus the results on the 0.9, 0.95, and 0.99 threshold, considering that below the 0.9 level, trends are clearly nonsignificant, whereas above the 0.99 level, the trend is well marked.

In the following, the hypothesis testing procedure described above has been applied to two different issues. Obviously, it has been used for evaluating the significance

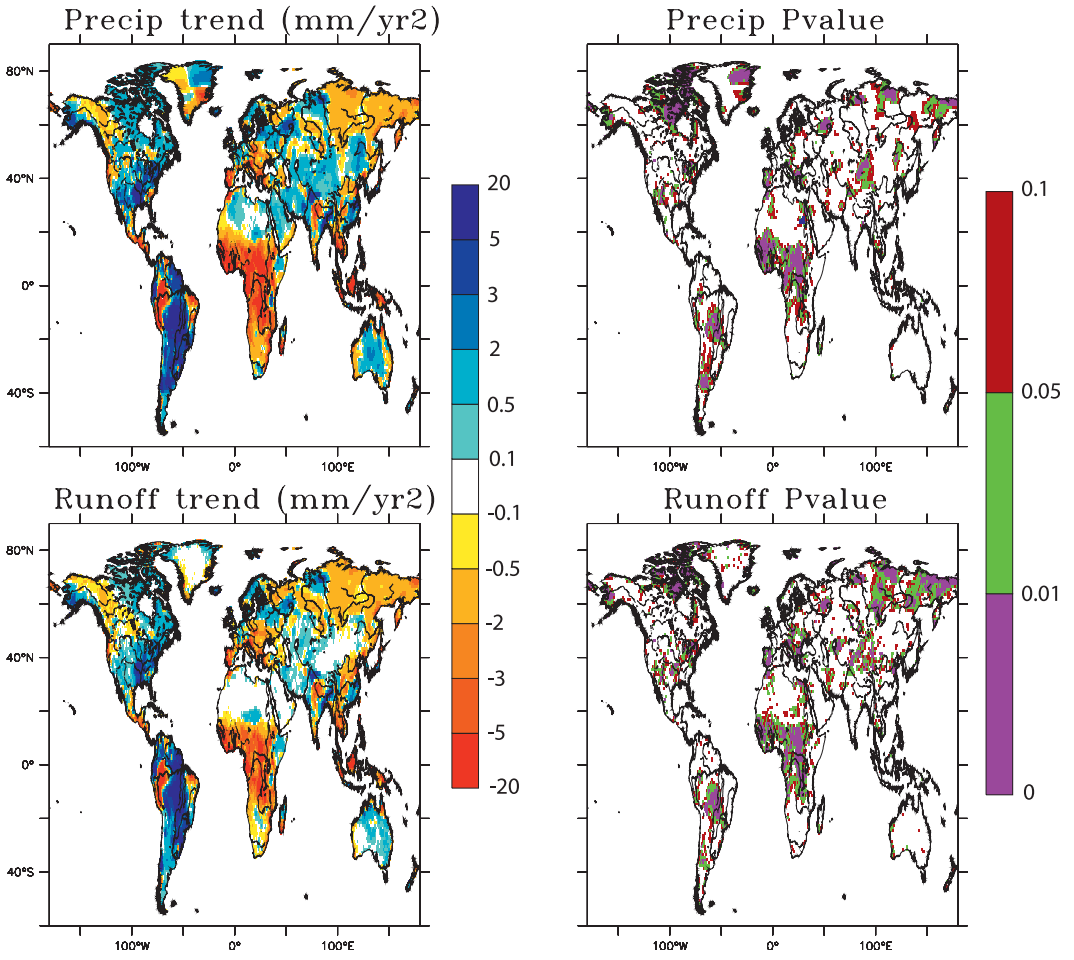

FIG. 2. (left) (top) Trends in GPCC land precipitation and (bottom) simulated runoff during the 1960–94 period. (right) The corresponding p values.

of observed or simulated trends. This technique has also been implemented for assessing differences between simulated and observed runoffs. In such a case, the y_i considered in the model equation (1) denotes, for the year i, the difference between the observed runoff and the simulated one. In other words, the comparison between observed and simulated trends has been made through (1) a direct comparison between observed and simulated runoff trends and (2) a comparison between observed and simulated p values. Such a methodology allows us to identify the river basins where the model behavior is significantly different from the observations and to address the question, is the simulated trend significantly different from the observed one? Two remarks must be made regarding this statistical analysis. First, the observation and model can be significantly different (i.e., the difference between observed and simulated runoffs shows a significant trend), whereas both ''individual'' trends are not significant. Second, the result of the test depends on both the difference in the trends and the model's ability to capture the observed interannual variability. In particular, if the model is highly accurate in this respect, then a small difference in the trends can be identified as significant.

3. Results

Figure 2 present the global distribution of the GPCC precipitation trends and the corresponding simulated runoff trends during the period 1960–94. The associated p value distribution is also shown. The simulated runoff trends show the same pattern and magnitude as the precipitation trends except over the arid areas, where runoff is negligible, given the balance between precipitation and surface evaporation. As indicated by the p values, the simulated runoff increases significantly over South and North America. In contrast, it decreases significantly over Africa, southern Europe, and eastern Siberia. Note that the p value is smaller for runoff than for precipitation

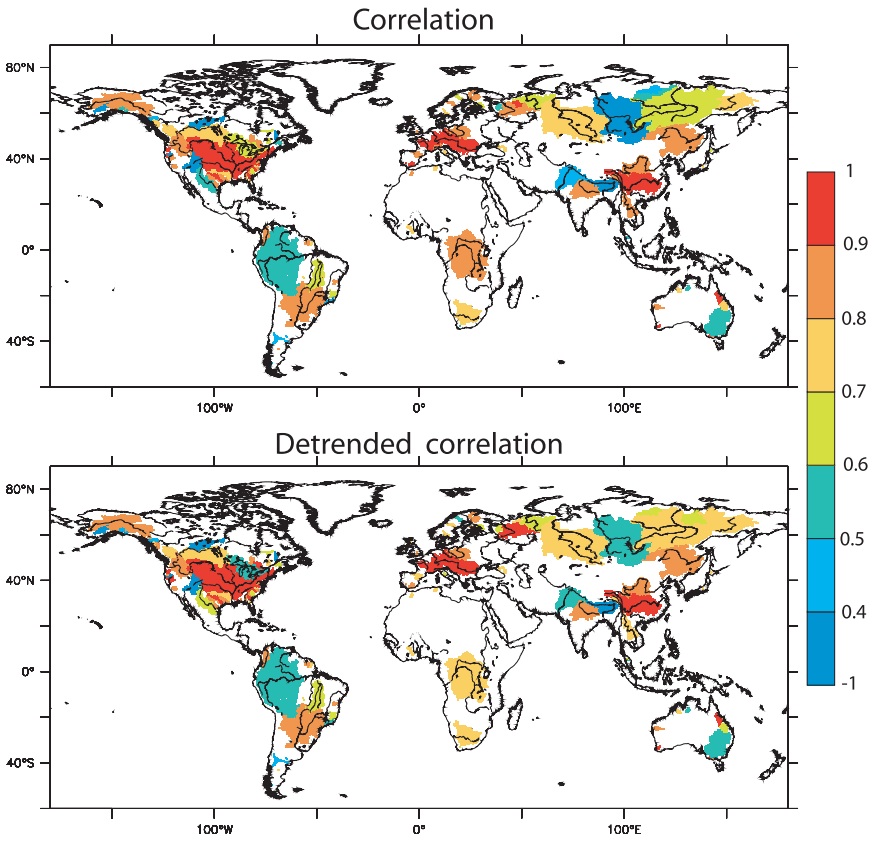

FIG. 3. (top) Correlations and (bottom) detrended correlation between observed and simulated annual mean discharges at each station given in Fig. 1.

over eastern Siberia, thereby suggesting a positive hydrological feedback and/or an alternate driving mechanism in this region.

Figure 3 presents the correlation and the detrended correlation between the observed and simulated discharges over the selected 154 river basins during the 1960–94 period. The interannual variability of observed annual mean discharge is generally well reproduced by ISBA-TRIP over these basins. The correlation between the observed and simulated values is generally more than 0.5. Some exceptions are found over Asia (Yenisei, Anabar, Indus, Brahmaputra), South America (Rio Negro), and North America (e.g., Kuskokwin, Churchill, Colorado). The Asian relative divergence is mainly due to contrasting multidecadal trends (Fig. 3). Indeed, Fig. 4 compares the observed and simulated annual mean time series over the largest 14 river basins. Results show a reasonable simulation of multidecadal trends except over the Yenisei, Lena, and Indus Rivers, where the simulated and observed trends are in opposition (Table 1). Despite obvious anthropogenic influences (dams and irrigation), the discharge simulated at the mouth of the Mississippi River is relatively close to the observations compared to the other rivers shown in Fig. 4. This might reflect the high rain gauge density and thereby the quality of the precipitation forcing over this basin.

In general, some important deficiencies appear, such as the general overestimation of the annual streamflow (except over boreal regions). Besides uncertainties in the precipitation forcing (e.g., Decharme and Douville 2006; Alkama et al. 2010a), this systematic error suggests an underestimation of surface evaporation that could be due to the lack of subgrid processes, such as evaporation at the potential rate over saturated areas (i.e., marshes, ponds, lakes, irrigated crops, and flood plains) (Decharme et al. 2008). These neglected processes can induce large errors, especially over dry regions, and consequently can affect the comparison between observed and simulated trends. This is particularly true in the case of the Indus River, in which the observed discharge shows damped interannual variability and negative trend compared to the simulated runoff and observed precipitation. Undoubtedly, neglecting irrigation in our experiment is a possible reason for this disagreement in the case of the Indus River but not for the east boreal basins (Lena, Yenisei).

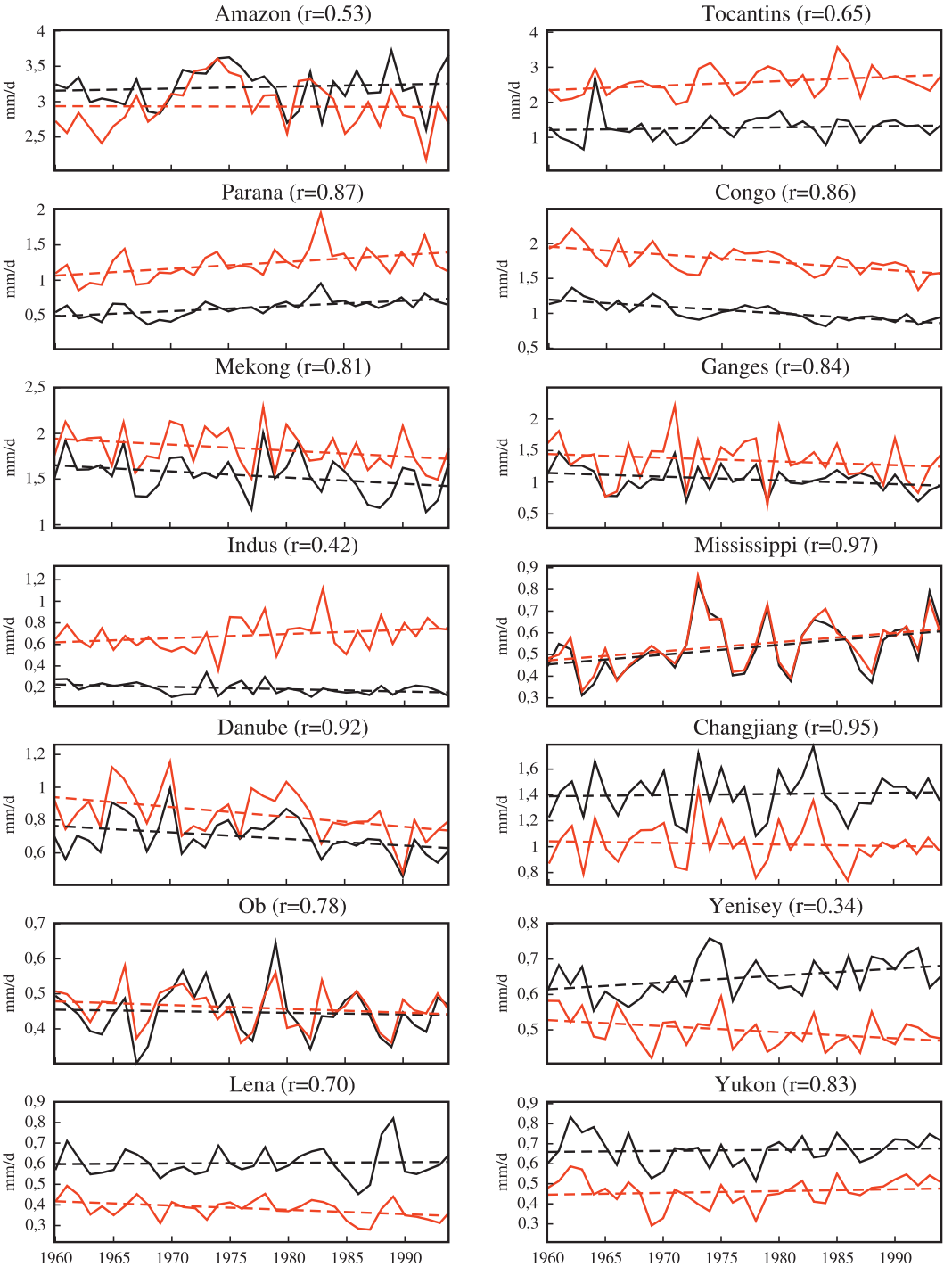

FIG. 4. Comparison between observed (black) and simulated (red) annual mean discharges for each basin given in Table 1. The corresponding correlations (r) and annual trends (dashed lines) are also shown. The trend values are given in Table 1.

Figure 5 compares the observed and simulated trends at the outlet of the 154 major river basins of the world selected for this study from Dai et al. (2009). At most stations, the model successfully captures the observed runoff trend, regarding the value of the trend and the corresponding statistical significance (that is illustrated by the p value). This agreement is particularly high over tropical regions. The main difference between the model

TABLE 1. Discharge characteristics during the 1965–1995 period at the downstream stations of the 14 rivers shown in Fig. 4: Drainage area (10^6 km^2) from observation (dr_{obs}) and simulation (dr_{sim}), the observed (Q_{obs}) and simulated (Q_{sim}) mean annual discharges (m^3 s^{-1}), its observed (t_{obs}) and simulated (t_{sim}) linear trend (mm yr^{-2}), and the p value of both observed (p_{obs}) and simulated (p_{sim}) linear trend. The significant trends at the 10% level are in bold.

River basins	Stations	dr_{obs}	dr_{sim}	Q_{obs}	Q_{sim}	t_{obs}	t_{sim}	p_{obs}	p_{sim}
Amazon	Obidos	4.62	4.70	1170	1070	1.07	0.08	0.54	0.96
Tocantins	Tucurui	0.74	0.79	465	937	1.35	**4.68**	0.55	**0.04**
Parana	Timbues	2.34	2.50	224	449	**2.65**	**3.54**	**0.01**	**0.01**
Congo	Kinshasa	3.47	3.75	375	643	**−3.59**	**−4.15**	**0.01**	**0.01**
Mekong	Paske	0.54	0.54	561	669	**−2.45**	**-2.36**	**0.06**	**0.07**
Gange	Farakka	0.95	0.91	382	491	**−2.14**	−2.14	**0.07**	0.32
Indus	Kotri	0.97	0.96	70	250	**−0.79**	1.42	**0.02**	0.11
Mississippi	Vicksburg	2.89	3.03	194	198	**1.65**	**1.55**	**0.03**	**0.03**
Danube	Ceatal	0.80	0.81	254	306	**−1.45**	**−2.18**	**0.03**	**0.01**
Changjiang	Datong	1.70	1.67	513	373	0.32	−0.44	0.76	0.65
Ob	Salekhard	2.43	2.82	163	168	−0.15	−0.38	0.71	0.26
Yenisei	Igarka	2.44	2.44	236	182	**0.71**	**−0.62**	**0.02**	**0.03**
Lena	Kusur	2.43	2.44	220	139	0.11	**−0.75**	0.81	0.01
Yukon	Pilot	0.83	0.82	244	168	0.18	0.33	0.69	0.44

and observations concerns the boreal river basins (mainly Asia), where the simulated runoff decreases, unlike observations (Table 1). Figures 5e and 5f also present the trend of the difference between the simulated and observed annual discharge and its corresponding p value. Results illustrate that the model shows few significant differences with observations over the tropics, except for some particular rivers (e.g., Indus and Chang Jiang), where neglecting irrigation in the ISBA-TRIP model seems to be the main reason for this disagreement. Indeed, Fig. 5g presents the global distribution of the irrigated area given by Siebert et al. (2005) (www.fao.org/nr/water/aquastat/irrigationmap/index10.stm), which shows that irrigation is intensive over South Asia, especially the Indus and Chang Jiang basins.

Instead, differences are often largely significant over the boreal region. This is particularly striking over eastern Siberia, where some important areas of permafrost are present, as shown by Fig. 5h. This global permafrost distribution is available online (http://nsidc.org/data/docs/fgdc/ggd318_map_circumarctic/index.html#5) (Brown et al. 2001). Several explanations can be put forth for this mismatch. First, the boreal region is the region where the rain gauge density is low and where the solid-to-total-precipitation ratio is high, so that the precipitation forcing is relatively uncertain. Second, relevant physical processes, such as the freeze–thaw cycle of permafrost (Fig. 5h) and the dynamics of glaciers, are still neglected in ISBA as in most other land surface models. This is an issue for the high-latitude hydrology, where the melting of permafrost and glaciers could be a significant source of additional freshwater discharge in the context of global warming (Serreze et al. 2002; Romanovskya et al. 2007; Surazakov et al. 2007; Adam and Lettenmaier 2008; Ye et al. 2009), as will be debated in the discussion section.

Figure 6 shows the trends in precipitation, as well as in the modeled and observed runoff during the 1960–94 period. The global averaged land precipitation (Po) and the corresponding simulated runoff (Rs) show negative trend. In contrast, the observed runoff at the outlet of the selected 154 large river basins RoD (about one-third of the total land area) shows an increase of ~0.16 mm yr^{-2}. One important remark is that the confidence intervals on these global variables are relatively large, so these estimated trends are far from being significant. Over the same area, the modeled runoff decreases by ~0.04 mm yr^{-2}. It is, however, necessary to focus on the continental and subcontinental scales to understand such a global mismatch. Figure 6 shows a relative consistency between the modeled and observed runoff trends over most continents, with the exception of Asia (where modeled and observed runoffs show opposite trends) and Europe (where the simulated trend is approximately 6 times larger than in observations). While this failure could be further evidence of the importance of the stomatal closure effect under increasing CO_2 concentration and/or of land use (not accounted for in our simulations), a more thorough analysis suggests another possible explanation. According to Fig. 5, the maximum mismatch is found in the high-latitude river basins. The 95% confidence interval in Fig. 6 indicates no significant global trends, neither in observed precipitation and runoff nor in simulated runoff. In contrast, a significant and consistent decrease (increase) is found over Africa (North and South America). Note that there are some similarities between our results (when averaged over 33% of the global land area) and the

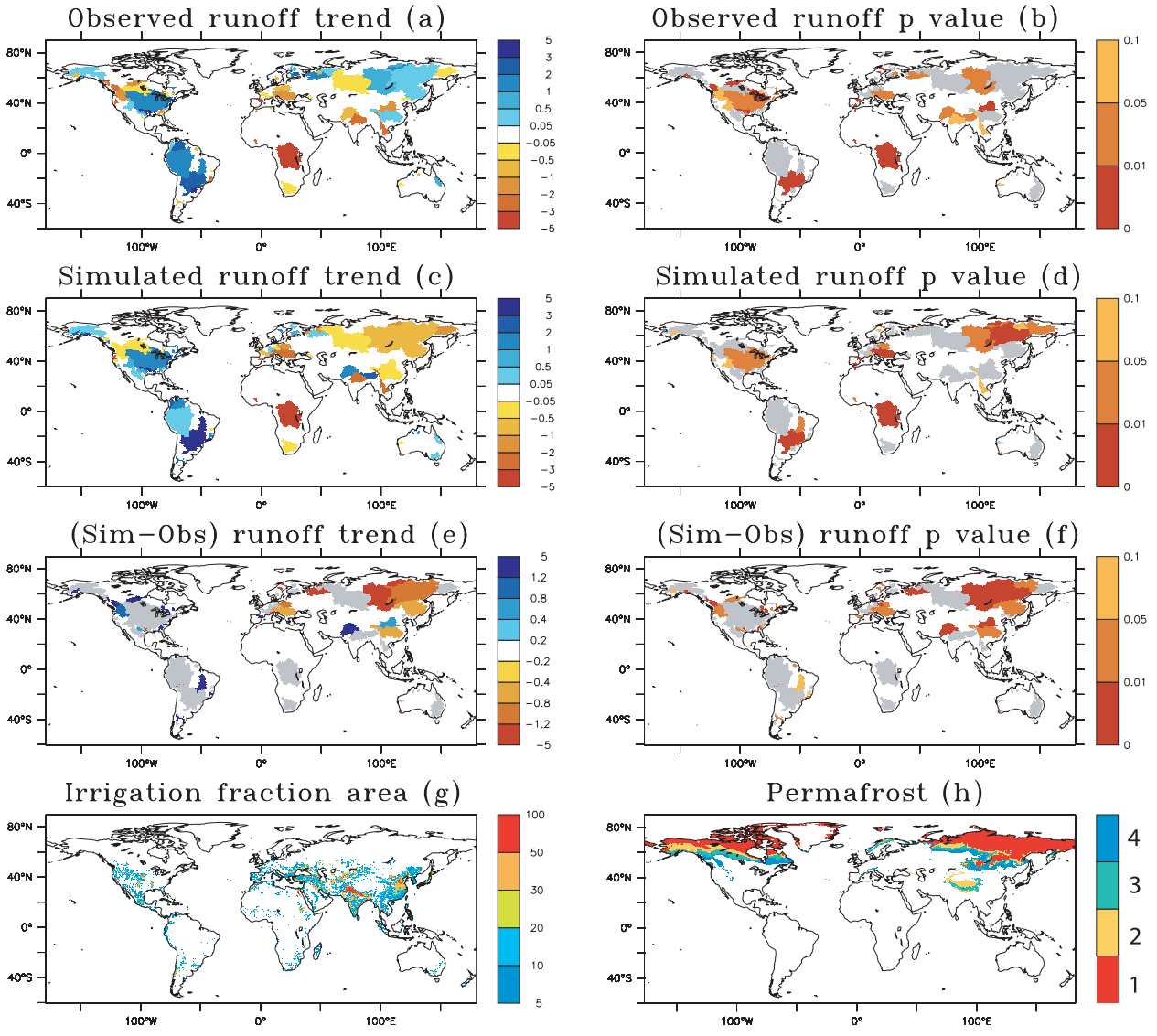

FIG. 5. Spatial distributions of (a) observed and (c) simulated annual runoff trends for each basin given in Fig. 1 and (b),(d) their corresponding p values, respectively. (e) The trend of the difference between simulated and observed annual runoff and (f) its corresponding p value if this p value is <0.1. (g) Percentile of the irrigated area is also shown as well as (h) the permafrost type distribution in which 1 correspond to continuous permafrost, 2 to discontinuous, 3 to sporadic, and 4 to isolated patches.

continent-by-continent runoff trends simulated by G06 when their experiment considers only climate variations and 20% of the global land area (Fig. 6). Such similarities but also the apparent discrepancies between both studies will be discussed in section 5.

To go one step further, Fig. 7 estimates the fraction of the global, European, and Asian land runoff trends explained by the rivers with outlets located north of 60°N. Results show that the northern basins are mainly responsible for the apparent mismatch between the model and observations. According to observations, the northern river basins explain 50% of the positive trend in global land runoff (Fig. 7). In contrast, over the same area, the modeled runoff shows a negative trend (Figs. 5 and 6). This result emphasizes the need for a more comprehensive modeling of cold processes before making any attempt to attribute the observed runoff trend to a direct (e.g., dams, stomatal closure) or indirect (e.g., global warming, anthropogenic aerosols) human influence.

4. Sensitivity to precipitation forcing

To test the sensitivity of the ISBA-TRIP model multidecadal variability, the full GPCC data product, which

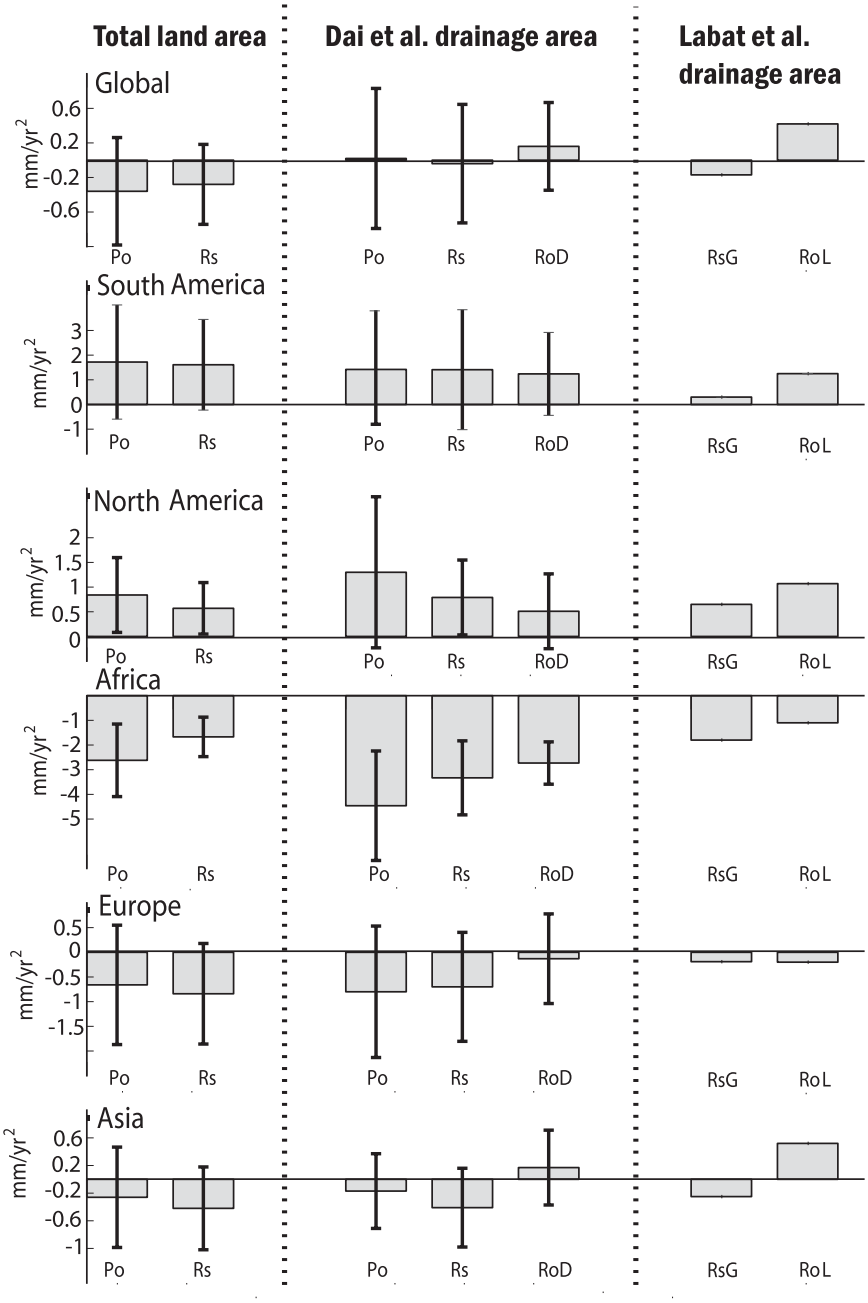

FIG. 6. Trends in Po and Rs for 6 regions: all land surfaces (global), South America, North America, Africa, Europe, and Asia. (left) A global average is shown, as well as (middle) RoD from Dai et al. (2009) and the corresponding drainage area average for precipitation and simulated runoff. (right) RoL from Labat et al. (2004) and RsG from G06 over the same drainage area as in Labat et al. (2004) (about 20% of the global land surface) are also provided.

is considered as a less homogeneous dataset, was also used. It is based on quality-controlled data from as many stations as possible with irregular coverage in time. It includes monthly data from about 10 000 to more than 40 000 stations, depending on the period—that is, the merged gauge dataset of the global collections of the Climatic Research Unit (CRU), FAO, National Climatic Data Center [NCDC; Global Historical Climatology Network (GHCN)], and all the national datasets delivered to the GPCC, together with the reprocessed real-time data. Thus,

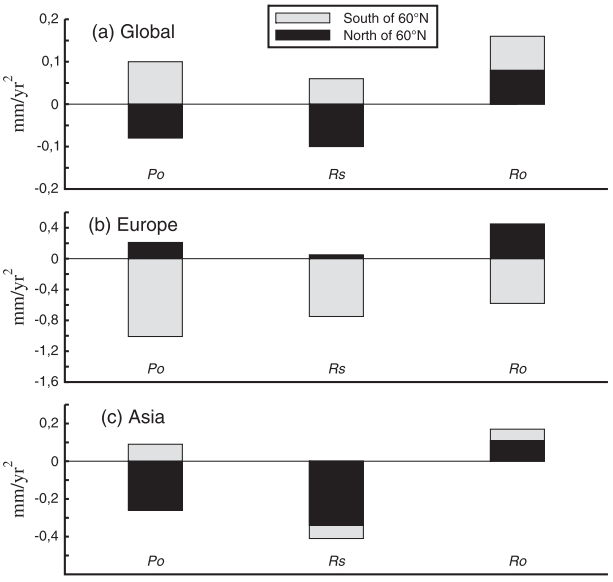

FIG. 7. The fraction of the (a) global, (b) European, and (c) Asian observed land runoff (Ro) and Po trends, as well as the Rs, explained by the rivers having outlets located north of 60°N (black) and south of 60°N (gray). Note that the sum of the southern and northern fractions is equal to the trends given in Fig. 6.

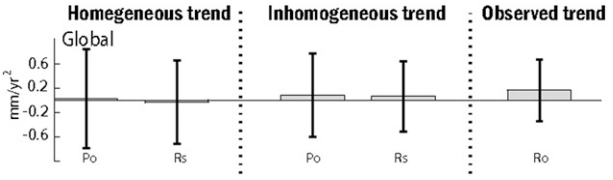

FIG. 8. Global trends of Ro and Rs land runoff using homogeneous and inhomogeneous GPCC Po.

the gridded dataset obtained is of much higher regional accuracy but is less recommended for trend analysis because of the varying data coverage with time.

Using this inhomogeneous precipitation forcing, the ISBA-TRIP model simulates a positive runoff trend over the selected 154 river basins (about 0.06 mm yr^{-2}), still weak but in line with the observed positive runoff trend (0.16 mm yr^{-2}) (Fig. 8). As in the observed and the homogeneous simulations, the inhomogeneous error bar shows no significant trend over the 154 rivers basin. Figure 9 shows that, south of 60°N, runoff interannual variability and trends simulated by the model are well reproduced, while this is not the case for river basins farther north. Not surprisingly, the interannual variability is slightly improved when using the inhomogeneous but more constrained precipitation forcing.

5. Discussion

The present numerical study suggests that the multidecadal variability of continental runoff over the second half of the twentieth century can be explained to a large extent without including the physiological effects of increasing CO_2 or changes in land use. The Ags version (Calvet et al. 1998) of ISBA does include a parameterization of the direct CO_2 effect on both stomatal closure and photosynthesis, but it was not activated in the present study. Preliminary tests with ISBA-Ags suggest a relative balance between stomatal closure and fertilization effects, and thereby confirm that such effects are highly model dependent (Alkama et al. 2010b). The impact of land use on the land surface hydrology is also unclear in former studies. On the one hand, when irrigation is neglected, land use can have a significant influence on runoff via a decrease in surface evapotranspiration (Piao et al. 2007). On the other hand, Liu et al. (2008) and Sun et al. (2008) indicate that deforestation over China, associated with irrigation, led to increased evapotranspiration over the twentieth century. However, Haddeland et al. (2007) found that regional irrigation effects were probably offset by land use change. Over the Mississippi River basin, Twine et al. (2004) suggest that deforestation acts to decrease evapotranspiration but that changing grasslands to croplands acts to increase it. Using the LPJmL model, Gerten et al. (2008) estimates the impact of irrigation on global twentieth-century runoff to be -1.1 km^3 yr^{-2}, which corresponds roughly to only 3% of the global simulated trend. Finally, using two different models, VanShaar et al. (2002) show that the impact of land use on the Columbia River hydrology is model dependent. In summary, the effect of land use on runoff is highly uncertain and is probably a regional rather than a global issue.

The larger difference between simulated and observed discharge trends appears over boreal regions. Over these basins, our hypothesis is that cold processes, poorly represented or even neglected in state-of-the-art land surface models, could be responsible for the contrast between observed and simulated runoff trends. Observational studies suggest that permafrost extent is shrinking and that the active layer thickness is increasing (Jorgenson et al. 2001; Serreze et al. 2002; Yang et al. 2002; Zhang et al. 2005). Permafrost represents an impermeable barrier to the vertical movement of liquid water in the soil: where permafrost is deep (and/or dense), thawing can increase soil water storage via a greater active layer thickness and thermokarst lake formation; conversely, thawing that promotes talik formation or removes barriers to groundwater flow may decrease soil water storage (Yoshikawa and Hinzman 2003; Smith et al. 2005). One of the direct consequences of shrinking permafrost is indeed the

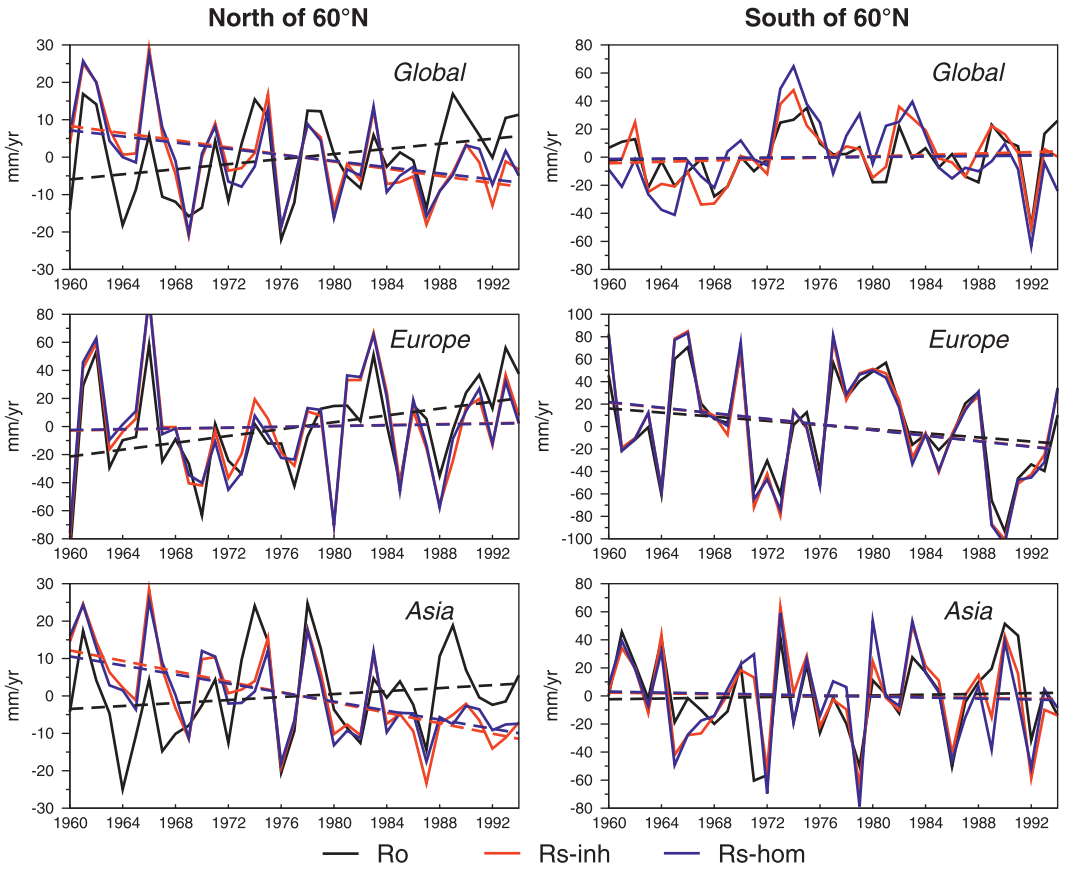

FIG. 9. Interannual variability (solid line) and trends (dashed line) in global, European, and Asian land runoff for basins (left) north of 60°N and (right) south of 60°N. The Ro (black), and the simulations with the inhomogeneous precipitation (Rs-inh, red) and with the homogeneous precipitation (Rs-hom, blue).

decline in lakes; permafrost can drain into the subsurface and thereby contribute to increased discharge into the surrounding rivers (Smith et al. 2005). In an observational study of major Eurasian rivers, Serreze et al. (2002) show that current runoff ratios (runoff/precipitation) are proportional to the extent of permafrost in basins. A degradation of permafrost may, therefore, have a significant impact on freshwater discharge to the Arctic Ocean (Serreze et al. 2002; Adam and Lettenmaier 2008). Runoff to the Arctic Ocean is already changing, reportedly increasing by 7% over the last 70 yr (Peterson et al. 2002).

Moving to methodological issues, G06 analyzed only the 1960–94 period and only over the drainage area for which the global runoff reconstructed by Labat et al. (2004) that is based on observations without gaps, roughly 20% of the total land surface area. In their simulation, driven only by climate forcings (neglecting stomatal conductance and land use effects), the continent-by-continent runoff trends are similar to our results, as shown in Fig. 6: only the Asian continent shows opposite trends between model and observations. Unfortunately, G06 averaged their results over the entire Asian continent and did not distinguish from the rivers that showed the maximum mismatch. Among the Asian rivers considered by Labat et al. (2004), only the Ob, Yenisei, and Lena are without gaps for the entire period of study (1960–94). However, permafrost is indeed quite extensive across the Lena and Yenisei basins, while only small part of northern Ob basin is covered by sporadic or discontinuous permafrost, as shown by Fig. 5h (Brown et al. 2001) and by other studies (Zhang et al. 2005; Ye and Fetzer 2009). As already stated, in the context of the late-twentieth-century global warming, the poleward retreat of permafrost could have contributed to the observed increase in runoff that is not captured by hydrological models. Such a hypothesis tempers the conclusion of G06, whereby "stomatal conductance is a major player on river runoff increase." Moreover, the precipitation dataset used by both G06 and Piao et al. (2007) is derived from the CRU climatology, which is based on a weaker density rain gauge network than the GPCC products used in the present

study. This could explain why, in Fig. 6, our simulated continental trends are generally closer to observations, except over Europe, compared to those of G06. The European exception is due to the inclusion of northern European rivers that were not considered by G06. Figures 7 and 9 of the present study show that the simulated runoff trend over southern Europe is close to the observed trend. Moreover, the results of the present study highlight that detection–attribution studies should not rely on global averages but rather focus on the latitudinal and/or regional distribution of hydrological variables (e.g., Zhang et al. 2007). The last methodological issue raised by the present study is the relevance of homogeneous (rather than heterogeneous as in former studies) precipitation forcings to analyze simulated runoff trends. Indeed, south of 60°N, the homogeneous simulation better reproduces the observed trend than the inhomogeneous simulation, except over Africa, where the number of in situ stations is very small and therefore not very representative in the homogeneous dataset (not shown). While such differences may not be significant, we argue that the development and use of homogeneous precipitation products can contribute to improving our understanding of runoff trends, at least at the regional scale.

6. Conclusions

After the original study by G06, who attributed a recent increase in global land runoff to the stomatal closure (reducing transpiration) response of plants to rising atmospheric CO_2, a number of both observational and numerical studies have led to different conclusions about this controversial issue. Using independent observations, Huntington (2008) provided evidence that transpiration has not decreased over recent decades, while Piao et al. (2007) attributed the twentieth-century runoff trends to both climate and land use changes. However, Gerten et al. (2008) emphasized the dominant contribution of the multidecadal variability of precipitation. Our study first suggests that such analyses can be misleading if particular attention is not paid to the use of a consistent and accurate definition of the simulated versus observed river drainage areas, and that such detection–attribution studies should rely on regional rather than global averages. Beyond multidecadal precipitation variability that seems to dominate the recent evolution of runoff in the tropics and midlatitudes, the study also emphasizes a possible human influence on high-latitude river discharge through the possible impact of global warming on permafrost and glaciers.

As far as the global terrestrial hydrological cycle is concerned, our results show no significant trend in both discharge and precipitation during the 1960–94 period. This is in agreement with Milliman et al. (2008) but in contradiction to claims of significantly increased twentieth-century river discharge (Probst and Tardy 1987; Labat et al. 2004; G06). Changes in individual rivers and at regional levels, however, have been noteworthy. This remark underlines the fact that runoff trends are a regional-scale and/or a basin-scale issue. Indeed, except high-latitude rivers and particular South Asian basins (e.g., Indus and Chang Jiang), where irrigation plays an important role, discharge trends are dominated by precipitation variability. Over high-latitude basins, beside uncertainties in precipitation, our hypothesis is that cold processes, poorly represented or even neglected in state-of-the-art land surface models, could be responsible for the contrast between observed and simulated runoff trends. How permafrost degradation impacts runoff to the Arctic Ocean remains an open question, but some observational evidence seems to show that this impact is significant (Serreze et al. 2002; Adam and Lettenmaier 2008). Indeed, over permafrost river basins, and especially over the Yenisei, both precipitation and discharge show significant but opposite trends. The increases in Yenisei River flow while precipitation decreases may be related to, among other factors, a degradation of permafrost (Serreze et al. 2002).

Combining in situ river discharge observations and runoff outputs of a land surface model, Dai et al. (2009) recently filled the gaps in the discharge time series of 925 large rivers and documented a small decline in global runoff over 1950–2000. Nevertheless, because of uncertainties in the observed precipitation forcing on the one hand and the lack of relevant physical processes on the other hand, such a strategy cannot be entirely trusted to fill the gaps in the observed time series, especially at high latitudes. Once again, our study suggests the need for improved parameterizations of cold processes in state-of-the-art land surface models and for accurate and homogeneous precipitation datasets in detection–attribution hydrological studies. Recent satellite observations, such as inundated areas (e.g., Decharme et al. 2008) and gravimetry (e.g., Alkama et al. 2010a; Decharme et al. 2010), could also be very useful to further constrain the models and lead to more robust conclusions about recent and future trends in continental runoff.

Acknowledgments. This work was supported by the CYMENT project of the RTRA STAE Toulouse and the IMPACT BOREAL project of the French ''Agence Nationale de la Recherche,'' with computer time provided by Météo-France. The authors wish to thank Dai et al. (2009) for their river discharge data collection effort as well as Taikan Oki for providing the original version of

the TRIP river routing model. Thanks are also due to the anonymous reviewers for their constructive comments.

REFERENCES

Adam, J. C., and D. P. Lettenmaier, 2008: Application of new precipitation and reconstructed streamflow products to streamflow trend attribution in northern Eurasia. *J. Climate,* **21,** 1807–1828.

Alkama, R., and Coauthors, 2010a: Global evaluation of the ISBA-TRIP continental hydrological system. Part I: Comparison to GRACE terrestrial water storage estimates and in-situ river discharges. *J. Hydrometeor.,* **11,** 583–600.

——, M. Kageyama, and G. Ramstein, 2010b: Relative contributions of climate change, stomatal closure, and leaf area index changes to 20th and 21st century runoff change: A modelling approach using the Organizing Carbon and Hydrology in Dynamic Ecosystems (ORCHIDEE) land surface model. *J. Geophys. Res.,* **115,** D17112, doi:10.1029/2009JD013408.

Beck, C., J. Grieser, and B. Rudolf, 2005: A new monthly precipitation climatology for the global land areas for the period 1951 to 2000. DWD Klimastatusbericht KSB 2004, 181–190.

Betts, R. A., and Coauthors, 2007: Projected increase in continental runoff due to plant responses to increasing carbon dioxide. *Nature,* **448,** 1037–1041.

Boone, A., J.-C. Calvet, and J. Noilhan, 1999: Inclusion of a third soil layer in a land surface scheme using the force–restore method. *J. Appl. Meteor.,* **38,** 1611–1630.

Brown, J., O. J. Ferrians, J. A. Heginbottom, and E. S. Melnikov, 2001: Circum-Arctic map of permafrost and ground-ice conditions. National Snow and Ice Data Center, Boulder, CO, digital media. [Available online at http://nsidc.org/data/ggd318.html.]

Calvet, J.-C., J. Noilhan, J.-L. Roujean, P. Bessemoulin, M. Cabelguenne, A. Olioso, and J.-P. Wigneron, 1998: An interactive vegetation SVAT model tested against data from six contrasting sites. *Agric. For. Meteor.,* **92,** 73–95.

Dai, A., T. Qian, K. E. Trenberth, and J. D. Milliman, 2009: Changes in continental freshwater discharge from 1948 to 2004. *J. Climate,* **22,** 2773–2791.

Decharme, B., 2007: Influence of runoff parameterization on continental hydrology: Comparison between the Noah and the ISBA land surface models. *J. Geophys. Res.,* **112,** D19108, doi:10.1029/2007JD008463.

——, and H. Douville, 2006: Introduction of a sub-grid hydrology in the ISBA land surface model. *Climate Dyn.,* **26,** 65–78.

——, and ——, 2007: Global validation of the ISBA sub-grid hydrology. *Climate Dyn.,* **29,** 21–37, doi:10.1007/s00382-006-0216-7.

——, ——, C. Prigent, F. Papa, and F. Aires, 2008: A new river flooding scheme for global climate applications: Off-line evaluation over South America. *J. Geophys. Res.,* **113,** D11110, doi:10.1029/2007JD009376.

——, R. Alkama, H. Douville, M. Becker, and A. Cazenave, 2010: Global evaluation of the ISBA-TRIP continental hydrological system. Part II: Uncertainties in river routing simulation related to flow velocity and groundwater storage. *J. Hydrometeor.,* **11,** 601–617.

Douville, H., J. F. Royer, and J. F. Mahfouf, 1995: A new snow parameterization for the Météo-France climate model. Part 1: Validation in stand-alone experiments. *Climate Dyn.,* **12,** 21–35.

——, D. Salas-Mélia, and S. Tyteca, 2006: On the tropical origin of uncertainties in the global land precipitation response to global warming. *Climate Dyn.,* **26,** 367–385, doi:10.1007/s00382-005-0088-2.

Gedney, N., P. M. Cox, R. A. Betts, O. Boucher, C. Huntingford, and P. A. Scott, 2006: Detection of a direct carbon dioxide effect in continental river runoff records. *Nature,* **439,** 835–838.

Gerten, D., S. Rost, W. von Bloh, and W. Lucht, 2008: Causes of change in 20th century global river discharge. *Geophys. Res. Lett.,* **35,** L20405, doi:10.1029/2008GL035258.

Haddeland, I., T. Skaugen, and D. P. Lettenmaier, 2007: Hydrologic effects of land and water management in North America and Asia: 1700–1992. *Hydrol. Earth Syst. Sci.,* **11,** 1035–1045.

Hansen, M. C., R. S. Defries, J. R. G. Townshend, and R. Sohlberg, 2000: Global land cover classification at 1 km spatial resolution using a classification tree approach. *Int. J. Remote Sens.,* **21,** 1331–1364.

Huntington, T. G., 2008: CO_2-induced suppression of transpiration cannot explain increasing runoff. *Hydrol. Processes,* **22,** 311–314, doi:10.1002/hyp.6925.

Jorgenson, M. T., C. H. Racine, J. C. Walters, and T. E. Osterkamp, 2001: Permafrost degradation and ecological changes associated with a warming climate in central Alaska. *Climatic Change,* **48,** 551–579.

Labat, D., Y. Goddéris, J. L. Probst, and J. L. Guyot, 2004: Evidence for global runoff increase related to climate warming. *Adv. Water Resour.,* **27,** 631–642.

Legates, D. R., H. F. Lins, and G. J. McCabe, 2005: Comments on ''Evidence for global runoff increase related to climate warming'' by Labat et al. 2004. *Adv. Water Resour.,* **28,** 1310–1315.

Liu, M., H. Tian, G. Chen, W. Ren, C. Zhang, and J. Lui, 2008: Effects of land-use and land-cover change the evapotranspiration and water yield in China during 1900-2000. *J. Amer. Water Resour. Assoc.,* **44,** 1193–1207.

Masson, V., J.-L. Champeaux, F. Chauvin, C. Meriguet, and R. Lacaze, 2003: A global database of land surface parameters at 1-km resolution in meteorological and climate models. *J. Climate,* **16,** 1261–1282.

Milliman, J. D., K. L. Farnsworth, P. D. Jones, K. H. Xu, and L. C. Smith, 2008: Climatic and anthropogenic factors affecting river discharge to the global ocean, 1951-2000. *Global Planet. Change,* **62,** 187–194.

Noilhan, J., and S. Planton, 1989: A simple parameterization of land surface processes for meteorological models. *Mon. Wea. Rev.,* **117,** 536–549.

Oki, T., and Y. C. Sud, 1998: Design of Total Runoff Integrating Pathways (TRIP)—A global river channel network. *Earth Interact.,* **2.** [Available online at http://EarthInteractions.org.]

Peterson, B. J., R. M. Holmes, J. W. McClelland, C. J. Vörösmarty, B. R. Lammers, A. I. Shiklomanov, I. A. Shiklomanov, and S. Rahmstorf, 2002: Increasing river discharge to the Arctic Ocean. *Science,* **298,** 2171–2173.

Piao, S., P. Friedlingstein, P. Cias, N. de Noblet-Ducoudré, D. Labat, and S. Zaehle, 2007: Changes in climate and land use have a larger direct impact than rising CO_2 on global river runoff trends. *Proc. Natl. Acad. Sci. USA,* **104,** 15 242–15 247.

Probst, J. L., and Y. Tardy, 1987: Long range streamflow and world continental runoff fluctuations since the beginning of this century. *J. Hydrol.,* **94,** 289–311.

Romanovskya, V. E., T. S. Sazonovaa, V. T. Balobaevb, N. I. Shenderb, and D. O. Sergueev, 2007: Past and recent

changes in air and permafrost temperatures in eastern Siberia. *Global Planet. Change,* **56,** 399–413.

Serreze, M. C., D. H. Bromwich, M. P. Clark, A. J. Etringer, T. Zhang, and R. Lammers, 2002: Large-scale hydro-climatology of the terrestrial Arctic drainage system. *J. Geophys. Res.,* **108,** 8160, doi:10.1029/2001JD000919.

Sheffield, J., G. Goteti, and E. F. Wood, 2006: Development of a 50-year high-resolution global dataset of meteorological forcings for land surface modeling. *J. Climate,* **19,** 3088–3111.

Siebert, S., P. Döll, J. Hoogeveen, J. M. Faures, K. Frenken, and S. Feick, 2005: Development and validation of the global map of irrigation areas. *Hydrol. Earth Syst. Sci.,* **9,** 535–547.

Smith, L. C., Y. Sheng, G. M. MacDonald, and L. D. Hinzman, 2005: Disappearing Arctic lakes. *Science,* **308,** 1429.

Soon, W. W.-H., D. R. Legates, and S. L. Baliunas, 2004: Estimation and representation of long-term (>40 year) trends of Northern-Hemisphere-gridded surface temperature: A note of caution. *Geophys. Res. Lett.,* **31,** L03209, doi:10.1029/2003GL019141.

Sun, G., C. Zuo, S. Lui, M. Lui, S. G. McNulty, and J. M. Vose, 2008: Watershed evapotranspiration increased due to changes in vegetation composition and structure under a subtropical climate. *J. Amer. Water Resour. Assoc.,* **44,** 1164–1175.

Surazakov, A. B., V. B. Aizen, E. M. Aizen, and S. A. Nikitin, 2007: Glacier changes in the Siberian Altai Mountains, Ob River basin, (1952–2006) estimated with high resolution imagery. *Environ. Res. Lett.,* **2,** 045017, doi:10.1088/1748-9326/2/4/045017.

Twine, T. E., C. J. Kucharik, and J. A. Foley, 2004: Effects of land cover change on the energy and water balance of the Mississippi River basin. *J. Hydrometeor.,* **5,** 640–655.

VanShaar, J. R., I. Heddeland, and D. P. Lettenmaier, 2002: Effects of land-cover changes on the hydrological response of interior Columbia River basin forested catchments. *Hydrol. Processes,* **16,** 2499–2520.

Yang, D., D. L. Kane, L. D. Hinzman, X. Zhang, T. Zhang, and H. Ye, 2002: Siberian Lena River hydrologic regime and recent change. *J. Geophys. Res.,* **107,** 4694, doi:10.1029/2002JD002542.

Ye, B., D. Yang, Z. Zhang, and D. L. Kane, 2009: Variation of hydrological regime with permafrost coverage over Lena basin in Siberia. *J. Geophys. Res.,* **114,** D07102, doi:10.1029/2008JD010537.

Ye, H., and E. J. Fetzer, 2009: Atmospheric moisture content associated with surface air temperatures over northern Eurasia. *Int. J. Hydrol.,* **30,** 1463–1471, doi:10.1002/joc.1991.

Yoshikawa, K., and L. D. Hinzman, 2003: Shrinking thermokarst ponds and groundwater dynamics in discontinuous permafrost near Council, Alaska. *Permafrost Periglacial Processes,* **14,** 151–160.

Zhang, T., and Coauthors, 2005: Spatial and temporal variability in active layer thickness over the Russian Arctic drainage basin. *J. Geophys. Res.,* **110,** D16101, doi:10.1029/2004JD005642.

Zhang, X., Z. W. Zwiers, G. C. Hegerl, F. H. Lambert, N. P. Gillett, S. Solomon, P. A. Stott, and T. Nozawa, 2007: Detection of human influence on twentieth-century precipitation trends. *Nature,* **448,** 461–466.